Novel Silver-doped $NiTiO_3$: Auto-combustion Synthesis, Characterization and Photovoltaic Measurements

S. Mostafa Hosseinpour-Mashkani, Mahnaz Maddahfar and Ali Sobhani-Nasab*

Young Researchers and Elites Club, Arak Branch, Islamic Azad University, Arak, Iran.

Received 24 March 2016, revised 26 July 2016, accepted 9 January 2017.

ABSTRACT

Novel silver-doped nickel titanate nanoparticles (Ag-$NiTiO_3$) were successfully prepared *via* a sol-gel method in the presence of stearyl alcohol as the capping agent and solvent. The formation of pure crystallized nickel titanate and silver-doped nickel titanate was occurred when the precursor was heat-treated at 700 °C in air for 150 and 60 min, respectively. The structural, morphological, and optical properties of obtained products were characterized by techniques such as X-ray diffraction (XRD), Fourier transform infrared (FT-IR) spectroscopy, Energy dispersive X-ray microanalysis (EDX), ultraviolet-visible (UV-vis), and scanning electron microscopy (SEM). The magnetic property of the prepared Ag-$NiTiO_3$ nanoparticles was also investigated with vibrating sample magnetometer (VSM). To fabricate a FTO/TiO_2/Ag-$NiTiO_3$/Pt-FTO solar cell, Ag-$NiTiO_3$ film was directly deposited on top of the TiO_2 prepared by electrophoresis deposition method. Furthermore, solar cell result indicates that an inexpensive solar cell could be developed by the synthesized Ag-$NiTiO_3$ nanoparticles.

KEYWORDS

Ag-$NiTiO_3$, sol-gel method, semiconductor, photovoltaic, doping.

1. Introduction

Nanomaterials have gained much attention among materials and their properties do not only depend on their composition but also on their shape and size distribution.[1–3] Functional inorganic metal titanate of the general formula $MTiO_3$ (M¼Pb, Ba, Sr, Ni, Fe, Zn, Cu, and Cr) has always been a topic of burgeoning interest largely because they display magnificent dielectric,[4] ferroelectric,[5] pyroelectrical,[6] piezoelectric,[7] magneto restrictive,[8] and electro-optical[9] characteristics. Such superior combination of functional properties ranked them as 'intelligent materials' for the development of sensors,[10,11] microelectronic devices,[12] and photocatalytic application.[13–14] Nickel titanate ($NiTiO_3$), a member of this well-known family, has a wide range of the above-mentioned properties, and has been extensively described in literature in crystal thin film and powder formats. $NiTiO_3$ is stable up to high temperature (1000 °C) even in air. Furthermore, the dielectric constant and magnetic susceptibility of $NiTiO_3$ is 13 K and 0.0096 X_m.[15] There are several methods for synthesizing pure nickel titanate material such as sol-gel,[16–17] polymeric precursor method,[18] electro spinning technique,[19] modified Pechini method,[20] etc. The sol-gel technique has many advantages over other fabrication techniques such as homogeneity, stoichiometry control, purity, ease of processing, controlling the composition, and ability to coat large and complex area substrates.[16] In this work, we report the synthesis of the pure Ag-$NiTiO_3$ nanoparticles *via* the sol-gel method using stearyl alcohol as the capping agent. This synthetic technique can easily be controlled and is more convenient for synthesis of pure mixed metal oxides nanoparticles. Furthermore, the possibility of developing a solar cell with ITO/Ag-$NiTiO_3$/TiO_2/Pt-ITO structure was also investigated.

2. Experimental

2.1. Characterization

X-ray diffraction (XRD) pattern was recorded by a Philips-X'PertPro (St Laurent, Quebec, Canada), X-ray diffractometer using Ni-filtered Cu Kα radiation at scan range of $10 < 2\theta < 80$ were used. The energy dispersive spectrometry (EDS) analysis was studied by XL30, Philips microscope (Phillips Company, Netherlands). Scanning electron microscopy (SEM) image was obtained on LEO-1455VP (Phillips, Amsterdam, Netherlands) equipped with an energy dispersive X-ray spectroscopy. Fourier transform infrared (FT-IR) spectra were recorded on Magna-IR, spectrometer 550 Nicolet with 0.125 cm^{-1} resolution in KBr pellets in the range of 400–4000 cm^{-1}. Photocurrent density-voltage (J-V) curve was measured by using computerized digital multimeters (Ivium-n-Stat Multichannel potentiostat) and a variable load. A 300 W metal xenon lamp (Luzchem) served as a simulated sunlight source, and its light intensity (or radiant power) was adjusted to simulated AM 1.5 radiation at 100 mW cm^{-1} with a filter for this purpose. The magnetic measurement of samples were carried out in a vibrating sample magnetometer (VSM) (Meghnatis Daghigh Kavir Co., Kashan Kavir, Iran) at room temperature in an applied magnetic field sweeping at ±10 000 Oe.

2.2. Synthesis of $NiTiO_3$ Nanoparticles

Nickel nitrate hexahydrate $Ni(NO_3)_2 6H_2O$, tetra-n-butyl titanate (TNBT), and stearyl alcohol used in experiments were all of analytical grade and used without any further purification. At first, 5 g of stearyl alcohol was melted in a beaker at 60 °C and then 0.34 g of nickel nitrate was added to the melted stearyl alcohol and stirring to form a transparent solution. Afterwards, 5 mL of TNBT was added to the above solution, stirring to form a homogeneous sol, naturally cooling down to room temperature, and drying in an oven for 12 h to obtain dried gel. Finally, the gel was calcined at 700 °C for 150 min in air to obtain $NiTiO_3$ nanoparticles.

2.3. Synthesis of Ag-$NiTiO_3$ Nanoparticles

In a typical synthesis procedure, the stoichiometric ratios of $NiTiO_3$ (1 mmol) and $AgNO_3$ (0.5 mmol) were dissolved in 30 mL of distilled water under magnetic stirring to form a homogeneous solution. Afterwards, the obtained precipitate was collected by

* To whom correspondence should be addressed. E-mail: ali.sobhaninasab@gmail.com

ISSN 0379-4350 Online / ©2017 South African Chemical Institute / http://saci.co.za/journal
DOI: http://dx.doi.org/10.17159/0379-4350/2017/v70a7

filtration and washed with absolute ethanol and distilled water several times. Finally, the precipitate was calcined at 700 °C for 60 min in air to obtain Ag-$NiTiO_3$ nanoparticles.

2.4. Cell Fabrication

Electrophoresis deposition (EPD) was utilized to the prepare TiO_2 films. During EPD, the cleaned FTO (Fluorine doped Tin Oxide) glass remained at a positive potential (anode) while a pure steel mesh was used as the counter (cathode) electrode. The linear distance between the two electrodes was about 3 cm. Power was supplied by a Megatek Pro-grammable DC Power Supply (MP-3005D). The applied voltage was 10 V. The deposition cycle was repeated 4 times, each time 5 s, and the temperature of the electrolyte solution was kept constant at 25 °C. The coated substrates were air-dried. The apparent area of the film was 1 × 1 cm. The resulting layer was annealed under air flow at 500 °C for 30 min. Electrolyte solution consisted of 120 mg L^{-1} of I_2, 48 mL L^{-1} of acetone, and 20 mL L^{-1} of water. For deposition of Ag-$NiTiO_3$ powder on the FTO glass substrate, a paste of Ag-$NiTiO_3$ was initially prepared. The slurry was produced by mixing and grinding 1.0 g of the nanometer sized Ag-$NiTiO_3$ with ethanol and water in several steps. Afterwards, the ground slurry was sonicated with ultrasonic horn (Sonicator 3000; Bandeline, MS 72, Germany) and then mixed with terpineol and ethyl cellulose as binders. After removing the ethanol and water with a rotary-evaporator, the final paste was prepared. The prepared Ag-$NiTiO_3$ paste was coated on TiO_2 film by a doctor blade technique. After that the electrode was gradually heated under an air flow at 450 °C for 30 min. Counter-electrode was made from deposition of a Pt solution on FTO glass. Afterwards, this electrode was placed over TiO_2/Ag-$NiTiO_3$ electrode. Sealing was accomplished by pressing the two electrodes together on a double hot-plate at a temperature of about 110 °C. The redox electrolyte consisting of 0.05 M of LiI, 0.05 M of I_2, and 0.5 M of 4-tert-butylpyridine in acetonitrile as a solvent was introduced into the cell through one of the two small holes drilled in the counter electrode. Finally, these two holes were sealed by a small square of sealing sheet and characterized by I-V test.

3. Results and Discussion

Crystalline structure and phase purity of as-prepared Ag-$NiTiO_3$ nanoparticles has been determined using XRD. The XRD pattern of Ag-$NiTiO_3$ nanoparticles is shown in Fig. 1. Figure 1 shows the formation of rhombohedral phase of $NiTiO_3$ (space group R-3, JCPDS No. 83-0198) along with cubic phase of Ag (JCPDS No. 87-0717). From XRD data, the crystallite diameter (Dc) of Ag-$NiTiO_3$ nanoparticle was calculated to be 18 nm using the Scherrer equation:[21]

$$D_c = K\lambda/\beta\cos\theta \quad (1)$$

where β is the breadth of the observed diffraction line at its half intensity maximum, K is the so-called shape factor, which usually takes a value of about 0.9, and λ is the wavelength of X-ray source used in XRD.

The morphology of the Ag-$NiTiO_3$ nanoparticles has been examined by SEM analysis (Fig. 2). According to the Fig. 2, it seems that the products mainly composed of small, spherical nanoparticles with average size of about 45 nm.

EDS analysis was used in order to evaluate the chemical composition and purity of final products, as shown in Fig. 3. The EDS spectrum of Ag-NiTiO3 nanoparticles shows the presence of Ni, Ti, Ag, and O elements in these nanoparticles. Furthermore, neither N nor C signals are detected in the EDS spectrum, which means the product is pure and free of any impurity.

The FT-IR spectrum of Ag-$NiTiO_3$ nanoparticles in the range 400–4000 cm^{-1} is shown in Fig. 4. The absorption band at 3424 cm^{-1} is attributable to the v(OH) stretching mode and the weak absorption band observed at 1741 cm^{-1} is due to the bending vibration of absorbed water[22] which indicates the presence of physisorbed water molecules linked to Ag-$NiTiO_3$ nanoparticles. Besides, the absorption band at 911 cm^{-1} belongs to the characteristic vibrations of the inorganic Ti-O-Ti network.[23] Furthermore, the absorption peaks at 536 and 685 cm^{-1} correspond to the Ti-O bending mode of TiO_2.[24] Moreover, the band at 446 cm^{-1} can be assigned to the absorption band of Ni-O, which confirms the formation of $NiTiO_3$.[14]

The diffused reflectance spectrum of the as-prepared Ag-$NiTiO_3$ nanoparticles is shown in Fig. 5. The fundamental absorption

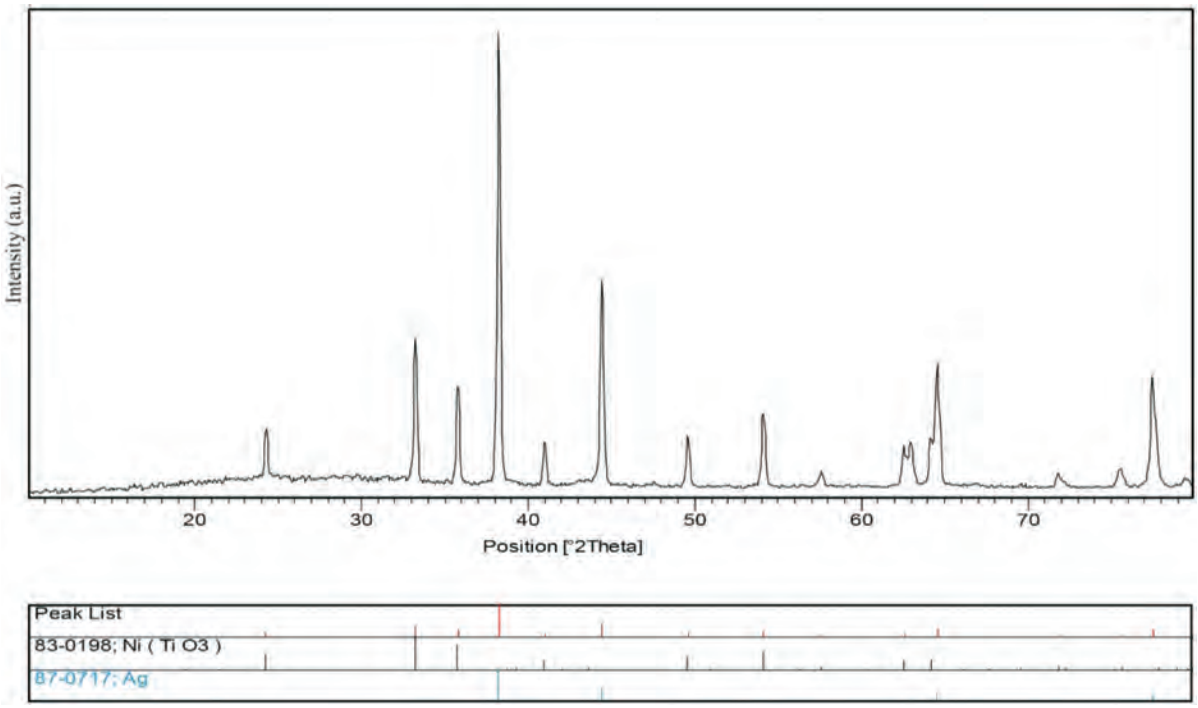

Figure 1 XRD pattern of Ag-$NiTiO_3$ nanoparticles calcined at 700 °C.

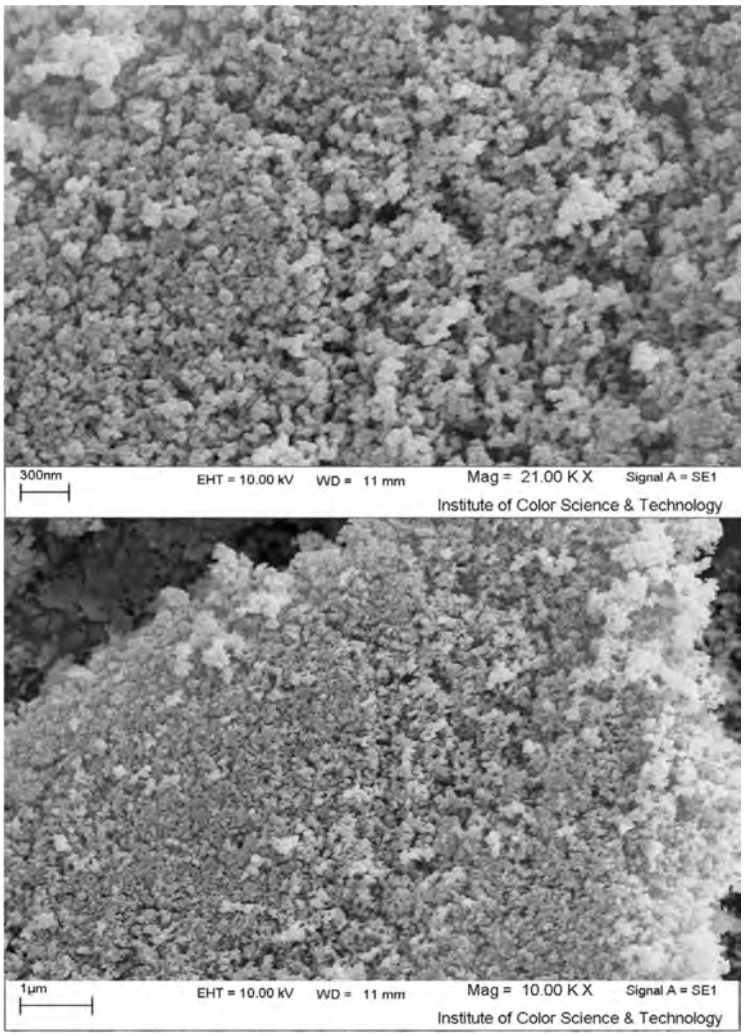

Figure 2 SEM image of Ag-$NiTiO_3$ nanoparticles calcined at 700 °C.

edge in most semiconductors follows the exponential law. Using the absorption data the band gap was estimated by Tauc's relationship:

$$\alpha = \alpha 0(h\nu - E_g)n/h\nu \quad (2)$$

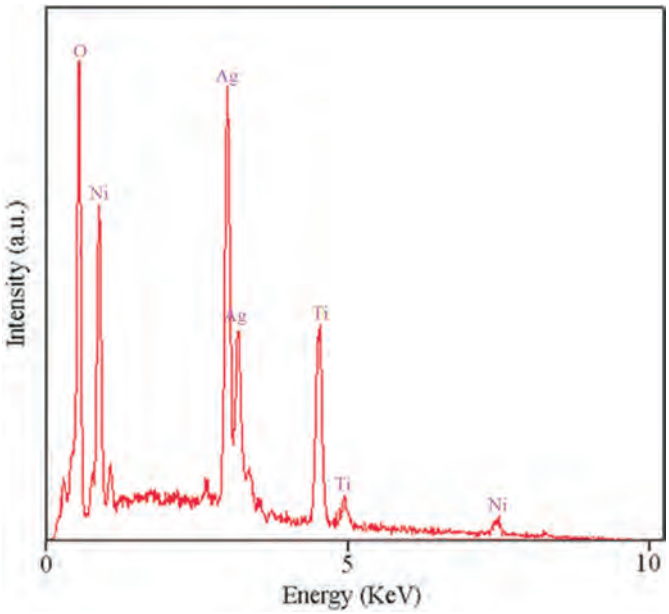

Figure 3 EDS pattern of Ag-$NiTiO_3$ nanoparticles calcined at 700 °C.

where α is absorption coefficient, hν is the photon energy, $\alpha 0$ and h are the constants, E_g is the optical band gap of the material, and n depends on the type of electronic transition and can be any value between 0.5 and 3. The energy gap of the Ag-$NiTiO_3$ nanoparticles is determined by extrapolating the linear portion of the plots of $(\alpha h\nu)^2$ against hν to the energy axis, as shown in Fig. 5. The E_g value is calculated as 2.1 eV for the Ag-$NiTiO_3$ nanoparticles which is lower than pure $NiTiO_3$ nanoparticles.[14] Moreover, the band gap of pure $NiTiO_3$ nanoparticles is slightly red shifted with add Ag on the surface of $NiTiO_3$. There is lowering of the band gap energy of the $NiTiO_3$ with add $AgNO_3$. This fall in band gap energy with add Ag might be due to the metallic clusters that introduce localized energy levels in the $NiTiO_3$ band gap. The electrons can be excited with lower energy from the valence band to these levels rather than to the conduction band of the semiconductor. Similar observations were also reported in literatures for Ag deposited semiconductor.[25,26]

I-V characterization of a typical solar cell fabricated using *in situ* approach is shown in Fig. 6. The measurement of the current density voltage (I-V) curve for Ag-$NiTiO_3$ was carried out under the illumination of AM1.5 (100 mW cm^{-2}). Device characteristics are as follows: V_{oc} = 0.3 V, J_{sc} = 0.167 mA cm^{-2}, FF = 3.2, and η = 0.16. In comparison with J-V characterization of $NiTiO_3$ nanoparticles,[14] dispersion of Ag over the surface of $NiTiO_3$ nanoparticles causes the surface plasmon resonance (SPR) and enhances the broad absorption in the entire visible region of the solar spectrum. Therefore, dispersion of Ag over $NiTiO_3$ nano-

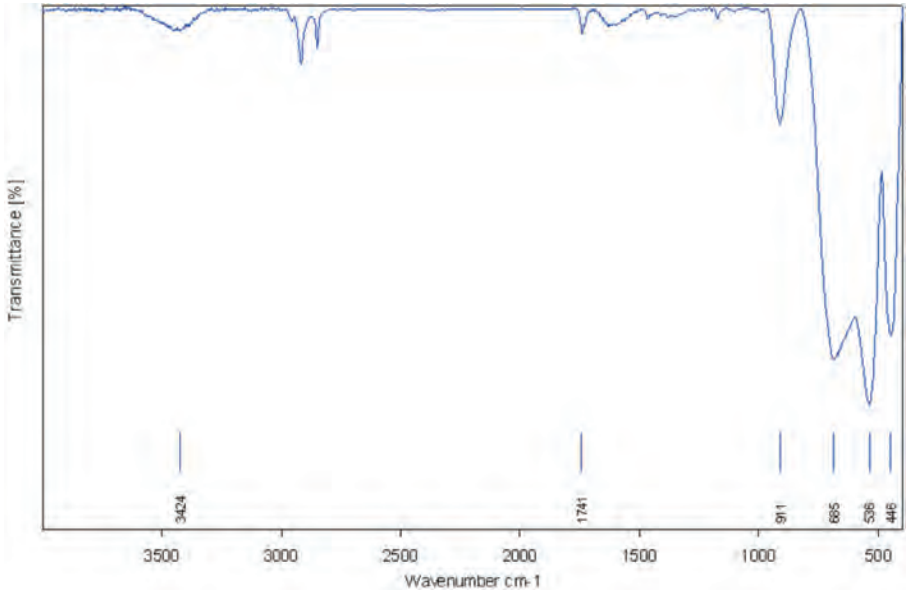

Figure 4 FT-IR spectrum of Ag-$NiTiO_3$ nanoparticles calcined at 700 °C.

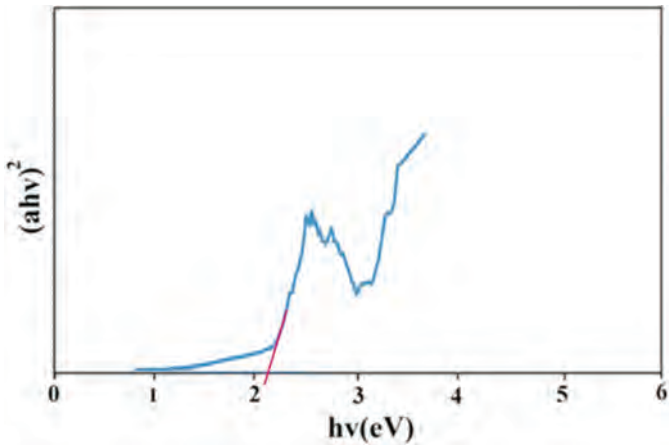

Figure 5 Diffuse reflectance spectrum of Ag-$NiTiO_3$ nanoparticles.

particles could be the better alternative to enhance the absorption of visible light by $NiTiO_3$ nanoparticles for effective solar cell.

The hysteresis loop of Ag-$NiTiO_3$ nanoparticles was studied to examine its magnetic properties (Fig. 7). According to the Fig. 7, at 300 K the remanent magnetization (Mr) is 0.002 emu g^{-1}, the coercive field (Hc) is 80 Oe, and the magnetization at saturation (Ms) is 0.06 emu g^{-1} (the saturation magnetization Ms was determined from the extrapolation of curve of H/M *versus* H).

4. Conclusions

In this work, Ag-$NiTiO_3$ nanoparticles were successfully synthesized *via* the sol-gel method. Stearyl alcohol played role as the capping agent and solvent. VSM result indicates a ferromagnetic behaviour for synthesized Ag-$NiTiO_3$ nanoparticles. A preliminary study on the possibility of developing a solar cell having FTO/TiO_2/Ag-$NiTiO_3$/Pt-FTO structure was also performed. Based on the VSM and photovoltaic measurement, magnetization at saturation (Ms) and conversion efficiency are 0.06 emu g^{-1} and $\eta = 0.16$, respectively. UV-Vis result confirmed the existence of strong plasmonic band induced by Ag nanoparticles *via* surface plasmon resonance. photovoltaic result was found to be significantly enhanced for the Ag doped $NiTiO_3$ caused due to the plasmonic resonance induced by $AgNO_3$.

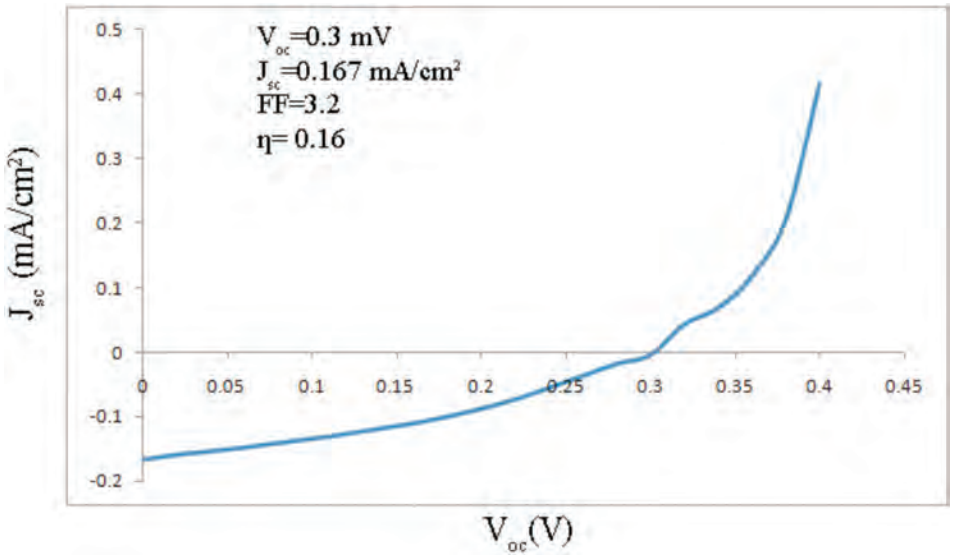

Figure 6 J-V characterization of Ag-$NiTiO_3$ nanoparticles calcined at 700 °C.

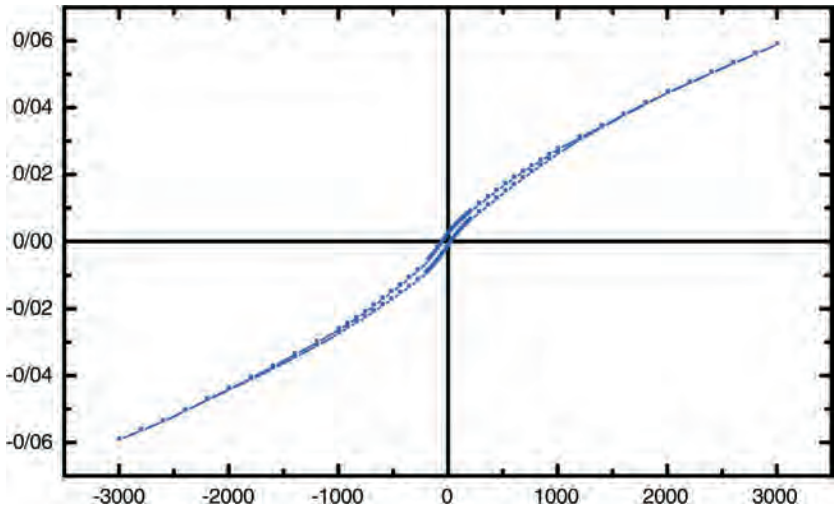

Figure 7 VSM curve of Ag-$NiTiO_3$ nanoparticles calcined at 700 °C.

Acknowledgement

Authors are grateful to council of University of Arak for providing financial support to undertake this work.

Conflict of Interest Statement

The authors declare that the research was conducted in the absence of any commercial or financial relationships that could be construed as a potential conflict of interest.

References

1 M. Ramezani, S.M. Hosseinpour-Mashkani, A. Sobhani-Nasab and H. Ghasemi-Estarki, Synthesis, characterization, and morphological control of $ZnMoO_4$ nanostructures through precipitation method and its photocatalyst application *J. Mater. Sci. Mater. Electron.*, 2015, **26**, 7588–7594

2 S.M. Hosseinpour-Mashkani, M. Ramezani, A. Sobhani-Nasab and M. Esmaeili-Zare, Synthesis, characterization, and morphological control of $CaCu_3Ti_4O_{12}$ through modify sol-gel method, *J. Mater. Sci. Mater. Electron.*, 2015, **26**, 6086–6091.

3 M. Maddahfar, M. Ramezani, M. Sadeghi and A. Sobhani-Nasab, $NiAl_2O_4$ nanoparticles: synthesis and characterization through modify sol-gel method and its photocatalyst application, *J. Mater. Sci. Mater. Electron.*, 2015, **26**, 7745–7750

4 T. Schneller, S. Halder, R. Waser, C. Pithan, J. Dornseiffer, Y. Shiratori, L. Houben, N. Vyshnavi and S.B. Majumder, Nanocomposite thin films for miniaturized multi-layer ceramic capacitors prepared from barium titanate nanoparticle based hybrid solutions, *J. Mater. Chem.*, 2011, **21**, 7953–7965.

5 A.I. Kingon and S. Srinivasan, Lead zirconate titanate thin films directly on copper electrodes for ferroelectric, dielectric and piezoelectric application, *Nat. Mater.*, 2005, **4**, 233–237.

6 B. Jaffe, *Piezoelectric Ceramics,* Elsevier, Netherlands, USA, 2012.

7 Y. Saito,H. Takao, T. Tani, T. Nonoyama, K. Takatori, T. Homma, T. Nagaya and M. Nakamura, Lead-free piezoceramics, *Nature*, 2004, **432**, 84–87.

8 J. Ma, Z. Shi and C.W. Nan, Magnetoelectric properties of composites of single $Pb(Zr,Ti)O_3$ rods and Terfenol-D/epoxy with a single-period of 1-3-type structure, *Adv. Mater.*, 2007, **19**, 2571–2573.

9 X. Wang, C.N. Xu, H. Yamada, K. Nishikubo and X.G. Zheng, Electro-mechano-optical conversions in Pr^{3+}-doped $BaTiO_3$-$CaTiO_3$ ceramics, *Adv. Mater.*, 2005, **17**, 1254–1258.

10 A. Bele, M. Cazacu, G. Stiubianu and S. Vlad, Silicone-barium titanate composites with increased electromechanical sensitivity, *RSC. Adv.*, 2014, **4**, 58522–58529.

11 Z. Lou, F. Li, J. Deng, L. Wang and T. Zhang, Branch-like hierarchical heterostructure (α-Fe_2O_3/TiO_2) A novel sensing material for trimethylamine gas sensor, *Appl. Mater. Interf.,* 2013, **5**, 12310–12316.

12 M. Lakshmi, A.S. Roy, S. Khasim, M. Faisal, K.C. Sajjan and M. Revanasiddappa, Dielectric property of $NiTiO_3$ doped substituted ortho-chloropolyaniline composites, *AIP Adv.,* 2013, **3**, 112–118.

13 A. Moghtada, A. Shahrouzianfar and R. Ashiri, Facile synthesis of $NiTiO_3$ yellow nano-pigments with enhanced solar radiation reflection efficiency by an innovative one-step method at low temperature, *Dyes Pigments*, 2013, **123**, 92–99

14 A. Sobhani-Nasab, S.M. Hosseinpour-Mashkani, M. Salavati-Niasari , H. Taqriri, S. Bagheri and K. Saberyan, Synthesis, characterization, and photovoltaic application of $NiTiO_3$ nanostructures via two-step sol-gel method, *J. Mater. Sci. Mater. Electron.*, 2015, **26**, 5735–5742.

15 Y. Ishikawa and S. Sawada, The study on substances having the ilmenite structure I. Physical properties of synthesized $FeTiO_3$ and $NiTiO_3$ ceramics, *J. Phys. Soc. Japan*, 1956, **11**, 496–501.

16 D.J. Taylor, P.F. Fleig and R.A. Page, Characterization of nickel titanate synthesized by sol-gel processing, *Thin Solid Films*, 2002, **408**, 104–110.

17 A.B. Gambhire, M.K. Lande, S.B. Kalokhe, A.B. Mandale, K.R. Patil, R.S. Gholap and B.R. Arbad, Synthesis and characterizations of $NiTiO_3$ nanoparticles prepared by the sol–gel process, *Philos. Mag. Lett.*, 2008, **88**, 467–472

18 K.P. Lopes, L.S. Cavalcante, A.Z. Simões, J.A. Varela, E. Longo and E.R. Leite, $NiTiO_3$ powders obtained by polymeric precursor method: synthesis and characterization, *J. Alloy. Compd.,* 2009, **468**, 327–332

19 N. Dharmaraja, H.C. Park, C.K. Kim, H.Y. Kim and D.R. Lee, Nickel titanate nanofibers by electrospinning, *Mater. Chem. Phys.,* 2004, **87**, 5–9.

20 Y.J. Lin, Y.H. Chang, W.D. Yang and B.S. Tsai, Synthesis and characterization of ilmenite $NiTiO_3$ and $CoTiO_3$ prepared by a modified Pechini method, *J. Non-Cryst. Solids,* 2006, **352**, 789–794.

21 D. Ghanbari, M. Salavati-Niasari, S. Karimzadeh and S. Gholamrezaei, Hydrothermal synthesis of Bi_2S_3 nanostructures and ABS-based polymeric nanocomposite, *J. NanoStruct.*, 2014, **4**, 227–232.

22 M. Goudarzia, D. Ghanbarib and M. Salavati-Niasaria, Room temperature preparation of aluminum hydroxide nanoparticles and flame retardant poly vinyl alcohol nanocomposite, *J. NanoStruct.*, 2015, **5**, 110–115.

23 N. Mir and M. Salavati-Niasari, Photovoltaic properties of corresponding dye sensitized solar cells: effect of active sites of growth controller on TiO_2 nanostructures, *Sol. Energy*, 2012, **86**, 3397–3404.

24 D. Wanga, L. Xiao, Q. Luo, X. Li, J. An and Y. Duan, Highly efficient visible light TiO_2 photocatalyst prepared by sol-gel method at temperatures lower than 300 °C, *J. Hazard. Mater.*, 2011, **192**, 150–159.

25 E. Pulido Melián, O. González Díaz, J.M. Doña Rodríguez, G. Colón, J.A. Navío, M. Macías and J. Pérez Peña, Effect of deposition of silver on structural characteristics and photoactivity of TiO_2-based photocatalysts, *Appl. Catal. B*, 2012, **127**, 112–120.

26 N. Sobana, M. Muruganadham and M. Swaminathan, Nano-Ag particles doped TiO_2 for efficient photodegradation of Direct azo dyes, *J. Mol. Catal. A*, 2006, **258**, 124–132.